International Journal of Innovative Computing, Information and Control
Volume **21**, Number **4**, August **2025**

ICIC International ©2025 ISSN 1349-4198
pp. **885–902**

IMPROVED LEADER-FOLLOWING FORMATION CONTROL FOR MULTI-DIFFERENTIAL-DRIVE AGV WITH OBSTACLE AVOIDANCE: VECTOR FIELD HISTOGRAM PLUS ALGORITHM

Huiyan Zhang[1,3,*], Yu Huang[2], Xiaoli Chen[3], Jiangyan Zou[3] and Wenting He[3]

[1]National Research Base of Intelligent Manufacturing Service
[2]School of Mechanical Engineering
[3]Chongqing Engineering Laboratory for Detection Control and Integrated Systems
Chongqing Technology and Business University
No. 19, Xuefu Avenue, Nan'an District, Chongqing 400067, P. R. China
{ huangyu201114; hewenting2000 }@163.com; chenxiaoli2@ctbu.edu.cn; jiangyanzou522@gmail.com
*Corresponding author: huiyanzhang@ctbu.edu.cn

Received December 2024; revised March 2025

Abstract. *This paper addresses the formation control problem for multi-differential-drive Automated Guided Vehicles (AGVs) incorporating obstacle avoidance via the Vector Field Histogram Plus (VFH+) algorithm. Specifically, leveraging the inherent characteristics of embedded control technology, we propose a novel path planning method for multi-differential-drive AGVs that demonstrates adaptability in dynamic environments, ensuring both real-time obstacle avoidance and robust formation maintenance. The proposed framework establishes global path planning through an indoor positioning system, complemented by local path planning combined with VFH+ algorithm and artificial potential field method. For formation control, we adopt a leader-follower approach combined with distributed sliding mode control, so that the multi-differential-drive AGV system can realize formation maintenance, obstacle avoidance, and collision prevention simultaneously. Finally, the effectiveness of the proposed algorithm is validated through comprehensive case studies involving a three-AGV formation performing obstacle avoidance.*
Keywords: Multi-differential-drive AGVs, Leader-follower formation control, VFH+ algorithm, Obstacle avoidance, Collision avoidance

1. **Introduction.** Over the past two decades, coordinated control of multi-mobile robot systems has emerged as a prominent research direction in the field of mobile robotics [1, 2, 3]. Among various collaborative strategies, formation control, as the most fundamental cooperative mechanism, has garnered substantial attention from the researchers [4]. However, with the increasing complexity of robotic tasks, the control objectives for multi-mobile robot systems have expanded beyond maintaining basic system stability and achieving formation adjustments. Contemporary research emphasizes safety aspects, including inter-robot collision prevention, obstacle-aware path planning, and comprehensive safety assurance. Consequently, the investigation of formation reconstruction, path planning, and obstacle avoidance mechanisms within the framework of multi-agent cooperation theory has progressively evolved into a burgeoning research domain [5, 6, 7].

The primary objective of formation control is to design effective control mechanisms that enable agents within a system to transition from initial states to a predefined configuration, while maintaining this formation throughout task execution. The scope of formation control research encompasses three fundamental aspects: formation generation,

DOI: 10.24507/ijicic.21.04.885

formation maintenance, and formation reconfiguration, each tailored to meet specific operational requirements. Historically, multi-agent formation control predominantly relied on centralized control architectures [8]; however, contemporary approaches have shifted toward distributed control methods. These distributed methodologies encompass several prominent strategies, including behavior-based approaches [9, 10], virtual structure methods [11], graph theory-based techniques [12, 13, 14], and leader-follower frameworks [15]. Among these, the graph theory-based method has gained prominence, which establishes a connection between formation stability and graph properties by incorporating rigid graph theory, resulting in both simplified analysis and increased flexibility. In this study, we employ a graph theory-based method to achieve triangular formation control. Nevertheless, practical implementation of formation control in real-world scenarios presents substantial challenges, particularly when multiple mobile robots encounter obstacles that disrupt their planned formation paths. Consequently, a critical challenge in formation control strategies lies in achieving coordinated obstacle avoidance while maintaining formation integrity and ensuring successful navigation to target destinations. This dual requirement of obstacle navigation and formation preservation has emerged as a significant research focus in the development of robust formation control strategies.

Numerous scholars have conducted extensive investigations into the aforementioned challenges, proposing various solutions. In [16], researchers developed a UAV obstacle avoidance method based on the fusion of ultrasonic and infrared rangefinder data. However, the reliance on low-cost sensors presents significant signal processing challenges, leading to suboptimal obstacle avoidance accuracy. Vargas et al. [17] tackled collision and obstacle avoidance in multi-agent systems through the implementation of soft and hard constraints within a distributed model predictive framework. A sampling-based trajectory planning approach for UAVs was introduced in [18], enabling real-time generation of obstacle avoidance paths between UAVs and dynamic obstacles, requiring a local path planning algorithm. Local path planning, commonly referred to as obstacle avoidance algorithms, currently encompasses several prominent algorithms, including the A* algorithm [19], ant colony optimization [20], artificial potential field methods [21], and Vector Field Histogram (VFH)-based approaches [22, 23]. In [24], researchers employed an integrated approach combining graph theory-based methods, leader-follower algorithms, and artificial potential field techniques to address formation control and obstacle avoidance challenges in complex environments. The study in [25] proposed a solution to inter-agent collisions through continuous repulsive vector fields, while [26] implemented a formation strategy for collision and obstacle avoidance utilizing vector histograms. However, as noted in [27], the implementation of these collaborative control methods in real-world multi-mobile robot systems faces significant challenges due to constraints imposed by robot encapsulation and existing controller, making it difficult to modify the controller directly for task adaptation. Consequently, the practical applicability of these methods in real-world scenarios remains questionable. Recent advancements in embedded control technology have emerged as a promising solution to these implementation challenges. [28] introduced a plug-and-play functionality for formation control of agents using this approach, while [27] built upon this work to address collision avoidance in multi-agent systems. Meanwhile, the authors mentioned that compared to the research on consensus problems addressed through embedded control technology [29], the related achievements in the field of formation control are relatively scarce.

With the ongoing development of intelligent manufacturing, the material handling sector has rapidly developed, leading to the widespread adoption of Automated Guided Vehicles (AGVs) in various material-intensive applications, including but not limited to

component assembly, parcel sorting, and dock operations [30]. Building upon the aforementioned research analysis, this paper investigates the formation collision avoidance problem in multi-differential-drive AGV systems using embedded control technology. The main contributions of this paper are summarized as follows.

1) A sliding mode control approach is developed for the kinematic model of AGVs, enabling effective formation control of multi-differential-drive AGVs through the integration of graph theory and distance constraint methods.
2) Compared with [27, 28], this paper implements the Vector Field Histogram Plus (VFH+) algorithm [31] to facilitate obstacle avoidance between AGVs and obstacles in complex environments. Furthermore, the repulsive field concept from artificial potential field methods is incorporated to prevent inter-AGV collisions during obstacle avoidance maneuvers.
3) A comprehensive joint experimental platform is established to validate the stability of the proposed control laws and demonstrate the effectiveness and practical applicability of the developed algorithms through embedded control technology implementation.

The remainder of this paper is structured as follows. Section 2 introduces the fundamental concepts of graph theory and establishes the necessary assumptions for AGV system modeling. Section 3 develops the kinematic model of AGVs and presents the corresponding control design. The theoretical framework and implementation of the formation collision avoidance algorithm are detailed in Section 4. Section 5 demonstrates the simulation results and experimental validation. Finally, Section 6 concludes this paper by summarizing the main contributions.

2. **Preliminaries and Problem Statement.** Consider a multi-agent system composed of N agents. The communication topology graph between the agents can be represented as $\zeta = (P, \varepsilon, A)$, where $P = \{p_1, \ldots, p_N\}$ denotes the set of nodes in the communication topology graph ζ; $\varepsilon = \{(i,j)|i,j \in P, i \neq j\}$ represents the set of edges in the communication topology graph ζ, and $A = [a_{ij}]_{N\times N}$ denotes the adjacency matrix. If and only if $(p_i, p_j) \in \varepsilon$ holds, then $a_{ij} > 0$, otherwise $a_{ij} = 0$. Define $N_i = \{j|(p_i, p_j) \in \varepsilon\}$ to represent the neighboring nodes of node i. The degree matrix $D = \operatorname{diag}\{d_1, \ldots, d_N\}$, $d_i = \sum_{j=1, j\neq i}^{N} a_{ij}$ of the communication topology graph ζ. The Laplacian matrix $L = [l_{ij}]_{N\times N} = D - A$ of the communication topology graph ζ, where $l_{ij} = \begin{cases} \sum_{j=1, j\neq i}^{N} a_{ij}, & i = j \\ -a_{ij}, & i \neq j \end{cases}$. If there exists a node that can reach any other node via a directed path, then the directed graph ζ is said to have a spanning tree.

In the leader-follower multi-agent system, the communication topology graph $\bar{\zeta} = \left(\bar{P}, \bar{\varepsilon}, A\right)$ describes the communication situation between agents, where $\bar{P} = \{p_0, p_1, \ldots, p_N\}$ represents the set of all nodes, with p_0 being the identifier of the leader and $p_1, \ldots, p_N$ being the identifiers of N followers. $\bar{\varepsilon} \subset \bar{P} \times \bar{P}$ represents the set of edges in the communication topology graph ζ, and the communication topology among followers can be represented by ζ. The communication matrix $C = \operatorname{diag}\{b_1, b_2, \ldots, b_N\} \in \mathbb{R}^{N\times N}$ between the leader and followers indicates that $b_i = 1$ means follower i can receive messages from the leader, while $b_i = 0$ indicates that follower i has no direct message exchange with the leader.

To ensure the feasibility of subsequent modeling and the convenience of calculations, while also improving control accuracy, the following assumption is necessary before describing the model [32].

Assumption 2.1. *Considering the model of the AGV used in this paper,*

1) *the hardware of the AGV is rigid, with special planar relationships that are strictly symmetric, parallel, or perpendicular;*
2) *the surface on which the AGV operates is flat, allowing the vehicle to move only in two-dimensional directions;*
3) *the wheels of the AGV maintain a tangent contact with the ground, rolling purely without slipping;*
4) *the effects of various resistances in the operating environment on the motion of the AGV are ignored.*

3. Kinematic Modeling and Control of AGVs.

3.1. Kinematic modeling of AGVs.

When describing the pose of the i-th two-wheeled driven AGV, it is necessary to establish two coordinate systems: one is the global coordinate system (XOY), and the other is the local coordinate system ($X_rO_rY_r$), as shown in Figure 1.

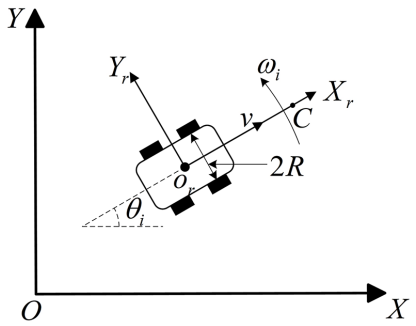

FIGURE 1. Diagram of the motion of a multi-differential-drive AGV

During motion, the velocity of the AGV's body at a certain moment of its centroid O_r can be expressed as $V_i = [v_i, \omega_i]^T$. In the control process, the mapping unit of the AGV system can map the body velocities v_i and angular velocity ω_i to the linear velocities v_r^i and v_l^i of the drive motors to control the movement of the vehicle. The mapping relationship can be expressed as

$$\begin{cases} v_r^i = \dfrac{v_i + \omega_i \times 2R}{2} \\ v_l^i = \dfrac{v_i - \omega_i \times 2R}{2} \end{cases} \tag{1}$$

In the two-dimensional global coordinate system, let $P_i = [x_i, y_i, \theta_i]^T$ be the pose vector of the AGV. The kinematic model of the AGV can be expressed as

$$\dot{P}_i = \begin{bmatrix} \dot{x}_i \\ \dot{y}_i \\ \dot{\theta}_i \end{bmatrix} = \begin{bmatrix} \cos\theta_i & 0 \\ \sin\theta_i & 0 \\ 0 & 1 \end{bmatrix} \begin{bmatrix} v_i \\ \omega_i \end{bmatrix} \tag{2}$$

Next, we establish the model for the pose error of the AGV, as shown in Figure 2. The point O_r represents the actual position of the centroid of the AGV, with its coordinates in the global coordinate system as $O_r(x_i, y_i)$ and the actual orientation as θ_i. Point C represents the corresponding desired position, with desired coordinates $C(x_r, y_r)$ and desired orientation θ_r^i. The pose error is obtained by calculating the differences in coordinates and angles between the two. By transforming the pose error coordinates to the local

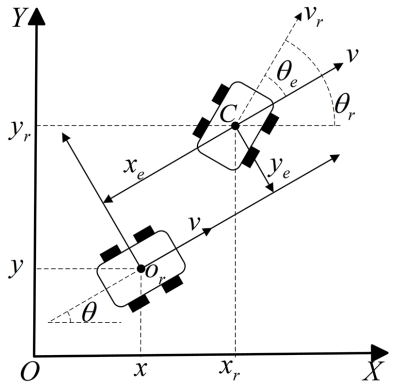

FIGURE 2. The model of the i-th AGV's pose error

coordinate system $X_rO_rY_r$, the pose error of the AGV, including the error along the X_r axis e_x^i, the error along the Y_r axis e_y^i, and the orientation error e_θ^i, can be expressed as

$$\begin{cases} e_x^i = (x_r^i - x_i)\cos\theta + (y_r^i - y_i)\sin\theta_i \\ e_y^i = -(x_r^i - x_i)\sin\theta + (y_r^i - y_i)\cos\theta_i \\ e_\theta^i = \theta_r^i - \theta_i \end{cases} \tag{3}$$

Then, define $e_P^i = \left[e_x^i, e_y^i, e_\theta^i\right]^T$ as the pose error vector of the AGV. The pose error of the AGV can be expressed as follows:

$$e_P^i = \begin{bmatrix} e_x^i \\ e_y^i \\ e_\theta^i \end{bmatrix} = \begin{bmatrix} \cos\theta_i & \sin\theta_i & 0 \\ -\sin\theta_i & \cos\theta_i & 0 \\ 0 & 0 & 1 \end{bmatrix} \begin{bmatrix} x_r^i - x_i \\ y_r^i - y_i \\ \theta_r^i - \theta_i \end{bmatrix} \tag{4}$$

At the same time, based on the kinematic differential equations, the pose error model of the AGV can be derived as follows:

$$\dot{e}_P^i = \begin{bmatrix} \dot{e}_x^i \\ \dot{e}_y^i \\ \dot{e}_\theta^i \end{bmatrix} = \begin{bmatrix} v_r^i \cos e_\theta^i - v_i + e_y^i \omega_i \\ v_r^i \sin e_\theta^i - e_x^i \omega_i \\ \omega_r^i - \omega_i \end{bmatrix} \tag{5}$$

3.2. **Kinematic sliding mode controller design of AGVs.** Sliding mode control is a distinct nonlinear control method characterized by its control law, which switches based on a real-time varying state feedback. This switching of output results is referred to as a "variable structure" process, with the ultimate goal of driving the system to follow predetermined requirements and dynamically approach the control target. The greatest advantage of sliding mode control is its robustness against both uncertainties within nonlinear systems and disturbances from the external environment [33]. Compared to other nonlinear control algorithms, the design process is also easier to implement. The formation path tracking system discussed in this paper is a typical nonlinear system; thus, we employ the sliding mode control algorithm to design the control law, using the pose error e_P^i during operation as the real-time feedback state, to output the AGV's forward velocity v_i and angular velocity ω_i.

The switching function design for the i-th AGV path tracking sliding mode controller is as follows:

$$s_i = \begin{bmatrix} s_1^i \\ s_2^i \end{bmatrix} = \begin{bmatrix} e_x^i \\ e_\theta^i + \arctan\left(v_r^i e_y^i\right) \end{bmatrix} \tag{6}$$

Introduce a constant speed reaching law for the above equation:

$$\dot{s}_i = \begin{bmatrix} \dot{s}_1^i \\ \dot{s}_2^i \end{bmatrix} = \begin{bmatrix} -k_1 \mathrm{sgn}\left(s_1^i\right) \\ -k_2 \mathrm{sgn}\left(s_2^i\right) \end{bmatrix} \tag{7}$$

where k_1 and k_2 serve as two sliding mode switching functions, each corresponding to the two control laws of the controller.

Based on Equations (2), (4)-(7), the control law for the AGV path tracking sliding mode controller can be obtained as follows:

$$u_i^v = \begin{bmatrix} u_1^i \\ u_2^i \end{bmatrix} = \begin{bmatrix} v_i \\ \omega_i \end{bmatrix} = \begin{bmatrix} e_y^i \omega + v_r^i \cos e_\theta^i + k_1 \mathrm{sgn}\left(s_1^i\right) \\ \dfrac{\omega_r^i + \frac{\partial \alpha}{\partial v_r^i} \dot{v}_r^i + \frac{\partial \alpha}{\partial e_y^i}\left(v_r^i \sin e_\theta^i\right) + k_2 \mathrm{sgn}\left(s_2^i\right)}{1 + \frac{\partial \alpha}{\partial e_y^i} e_x^i} \end{bmatrix} \tag{8}$$

where $\frac{\partial \alpha}{\partial v_r^i} = \frac{e_y^i}{1+(v_r^i e_y^i)^2}$, $\frac{\partial \alpha}{\partial e_y^i} = \frac{v_r^i}{1+(v_r^i e_y^i)^2}$.

4. Formation Control Strategy with Collision and Obstacle Avoidance.

4.1. **Formation control strategy.** This paper utilizes a distance constraint mechanism to ensure that the two AGV followers maintain fixed relative positions with respect to the AGV leader, thereby achieving the formation goal. Then, the formation controller is designed as

$$u_i^f = \sum_{j=1}^{N} a_{ij} * \left(p_j - p_i - l_{ij}\right) \tag{9}$$

where $N = 2$, p_i represents the coordinates of the AGV leader as $[x_i, y_i, 0]^T$, and p_j denotes the position coordinates of the AGV leader as $[x_j, y_j, 0]^T$, $l_{21} = [-\gamma_x d, -\gamma_y d, 0]^T$ and $l_{31} = [-\gamma_x d, \gamma_y d, 0]^T$.

To ensure that the multi-differential-drive AGVs can accomplish formation control tasks, our experimental AGVs must possess accurate tracking of position, velocity, and orientation. They should be able to follow predetermined trajectories and targets accurately and stably in dynamic environments through control algorithms. Additionally, we have designed a guidance module to calculate the desired position and expected yaw angle for the AGV based on its current position and target position. In this way, the robots gradually achieve the predetermined formation control tasks in real-world multi-differential-drive AGVs, ultimately completing the desired formation shape accurately. Throughout the process, the robots adjust their positions and orientations progressively using effective control algorithms, ensuring that they maintain the required formation and meet the task requirements.

4.2. **Collision avoidance strategy.** To achieve collision avoidance between agents and ensure the smooth completion of formation obstacle avoidance tasks, we need to incorporate appropriate collision avoidance algorithms into the control of individual AGVs. Specifically, we utilize the artificial potential field method to establish a suitable potential function, driving the AGVs to move along the negative gradient of the potential function until the control objectives are met. Each AGV is treated as a high potential field, generating repulsive forces when the distance between two AGVs is either too small or too large, thereby causing the AGVs to move apart or come closer, ultimately ensuring collision avoidance.

As shown in Figure 3, a collision avoidance region is defined for each AGV based on the artificial potential field method. When other AGVs enter this collision avoidance region, a repulsive force function is triggered, causing AGVs at risk of collision to repel each

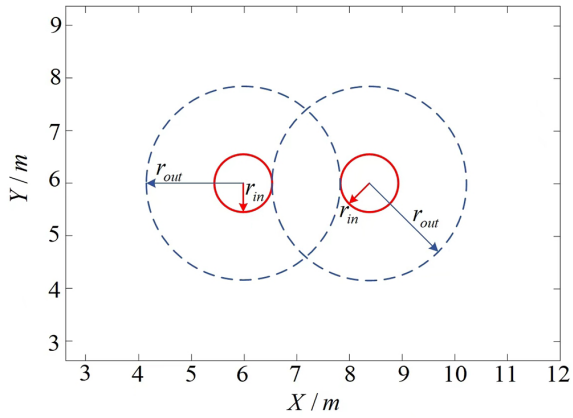

FIGURE 3. Collision avoidance area of the AGV

other, achieving collision avoidance. Considering the rigid area and physical inertia of the AGVs, let r_{in} represent the radius of the AGV's rigid body and r_{out} represent the range of the repulsive force field. When the distance between AGV agents i and j satisfies $\|d_{ij}\| = \|d_i - d_j\| \leq r_{out}$ and $d_i = \sqrt{x_i^2 + y_i^2}$, agent j is defined as a collision avoidance neighbor of agent i, denoted as $j \in N_i^r$. This can be defined as $N_i^r = \{j : \|d_i - d_j\| \leq r_{out}\}$.

Based on the artificial potential field method, we design a repulsive force function $\Lambda(\|d_{ij}\|)$ to ensure that when agent i enters the collision avoidance region of agent j, it experiences a repulsive force, causing agent i to move away from agent j and thereby achieve collision avoidance between agents. The construction of the repulsive force function is as follows:

$$\Theta = \begin{cases} a_r = \exp(k * \|d_{ij}\|) \\ \vec{v}_r = a_r * \text{normalize}(p_i - p_j) \end{cases} \tag{10}$$

$$\Lambda(\|d_{ij}\|) = \begin{cases} \Theta, & 2r_{in} \leq \|d_{ij}\| \leq r_{out} \\ 0, & \text{others} \end{cases} \tag{11}$$

where $\exp(k * \|d_{ij}\|)$ represents the exponential function with base e, k is the decay coefficient and a_r denotes the magnitude of the repulsive force. $\text{normalize}(p_i - p_j)$ represents the unit vector pointing from agent i to agent j, and $\vec{v}_r$ indicates the repulsive force vector acting on agent i.

Then, the collision avoidance controller is designed as

$$u_i^c = \sum_{N}^{i=1,j=1} a_{ij} * \Lambda(\|d_{ij}\|) \tag{12}$$

In summary, the multi-differential-drive AGV system now has formation and collision avoidance capabilities, so the input for the i-th AGV is

$$\begin{cases} u_i = u_i^v + u_i^c, & i = \text{leader} \\ u_i = u_i^v + u_i^c + u_i^f, & i = \text{otherwise} \end{cases} \tag{13}$$

Remark 4.1. *In (13), task commands are transmitted from the host computer to the leader, who then conveys its information to the following AGVs with which it communicates. Thus, the formation input u_i^f enables followers to acquire the leader's information to establish the formation, while u_i^v ensures the kinematic stability of each AGV.*

4.3. **Obstacle avoidance strategy.** Given that multi-differential-drive AGV systems frequently encounter obstacles in dynamic environments, this paper adopts the VFH+

algorithm as the local path planning algorithm. Compared with VFH, the VFH+ algorithm incorporates the robot's size and minimum safe distance into its model during the iterative process, resulting in paths that are more stable and smoother. Consequently, the trajectory obtained is superior to that of the original VFH algorithm [31]. The VFH+ algorithm uses a grid map to represent the Certainty Value (CV) of the presence of obstacles. A high CV value indicates a greater likelihood of obstacles being present. The size of the CV value c_{ij} for each grid can be determined using empirical equations. The specific implementation steps of the VFH+ obstacle avoidance algorithm are as follows.

Step 1: To program the AGV with a laser radar system for scanning information about dynamic obstacles around it, the scanning area of 360 degrees will be divided into n small sectors according to the radar resolution f (for example, $n = 360/f$). Each sector will be numbered from 0 degrees to 360 degrees (e.g., Q_l where $l < n$ and $l \in \mathbb{N}^+$, with l representing the sector number). For the obstacle information detected by the laser radar, we will calculate the Euclidean distance d^* from the AGV to the obstacle as follows:

$$d^* = \sqrt{(x_{\text{obs}} - x_{\text{AGV}})^2 + (y_{\text{obs}} - y_{\text{AGV}})^2}$$

and the angle α as

$$\alpha = \arctan\left(\frac{y_{\text{obs}} - y_{\text{AGV}}}{x_{\text{obs}} - x_{\text{AGV}}}\right), \quad \alpha \in [0, 2\pi]$$

Then, based on the angular orientation between the obstacle and the laser radar, we can assign the obstacle to the corresponding small sector (e.g., $l = \text{round}(\alpha/f)$, where "round" indicates rounding to the nearest integer). This way, all obstacles can be classified into their corresponding sectors. In dense environments where multiple obstacles may exist in the same sector, the minimum distance d^*_{min} to the closest obstacle will be taken as the obstacle distance for that sector. Thus, the obstacle distance for each sector can be represented as D_l (where $l < n$ and $l \in \mathbb{N}^+$), that is, $D_l = d^*_{\text{min},l}$, $(l < n,\ l \in \mathbb{N}^+)$.

Step 2: According to the vectorization formula of the VFH+ algorithm, the obstacle intensity value m_l for each sector can be calculated as follows:

$$m_l = c_v^2 \left(a - bD_l^2\right)$$

where m_l represents the obstacle intensity value for the l-th sector. A larger m_l indicates a greater danger from obstacles in that sector to the unmanned vehicle, meaning the obstacles are closer to the vehicle. The constants c_v^2, a, and b are defined such that $a = bD^2_{\text{max}}$.

Step 3: Feasibility sector analysis involves setting a threshold M to evaluate the safety credibility of each sector. The credibility for passage through each sector can be expressed as follows:

$$H_l = \begin{cases} 0 & \text{if } m_l \le M \\ 1 & \text{if } m_l > M \end{cases}$$

where H_l represents the passability of the l-th sector, with 0 indicating that it is safe to pass and 1 indicating danger, meaning it is not safe to pass.

Step 4: After performing passability analysis on all sectors, it is necessary to optimize the feasible sectors to find the optimal obstacle avoidance direction ϑ. This requires a suitable cost function to evaluate these candidate directions ϑ_l and select the avoidance direction ϑ, expressed as follows:

$$C(\vartheta) = \mu_1|\vartheta - \vartheta_{\text{goal}}| + \mu_2|\vartheta - \vartheta_{\text{current}}| + \mu_3|\vartheta - \vartheta(t-1)|$$

where $|\vartheta - \vartheta_{\text{goal}}|$ represents the angle between the candidate direction and the AGV's goal direction; $|\vartheta - \vartheta_{\text{current}}|$ represents the angle between the candidate direction and the AGV's current motion direction; and $|\vartheta - \vartheta(t-1)|$ represents the angle between the candidate direction and the AGV's previous motion direction. The coefficients μ_1, μ_2 and μ_3 correspond to the respective weights. The direction with the minimum cost value from $C(\vartheta)$ will be chosen as the obstacle avoidance direction.

5. **Simulation Results.** The effectiveness of the method is validated by adopting the communication topology shown in Figure 4. Using graph theory to represent the communication between AGVs, the adjacency matrix A is given by

$$A = \begin{pmatrix} 0 & 0 & 0 \\ 1 & 0 & 0 \\ 1 & 0 & 0 \end{pmatrix}$$

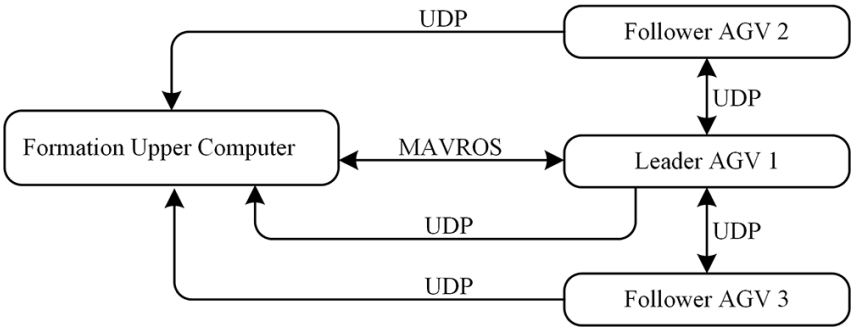

FIGURE 4. Communication status of the AGV

In the communication topology shown in Figure 4, the formation upper computer communicates with the leader using the MAVROS protocol. It publishes the formation task to the leader and subscribes to the leader's status for formation task management and status monitoring. The leader continuously sends its position to the followers in real time as the desired input for the formation control of master-slave multi-differential-drive AGVs. The AGVs publish their position data to the followers, and the followers update their own positions according to Equation (9), completing the real-time formation. Throughout the entire formation process, the status of each AGV is sent via UDP to the ground station for monitoring, ensuring the reliability of the formation algorithm results presented in this paper.

5.1. **Numerical example.** To validate the effectiveness of the distance constraint mechanism and the VFH+ algorithm (as shown in Table 1) in formation-based obstacle avoidance, the initial position vectors P_i of the unmanned vehicles in Equation (2) are set as $P_1 = [0, 0, 0]^T$, $P_2 = [-5, 5, 0]^T$, and $P_3 = [5, -5, 0]^T$, where P_1 represents the leader and the others are the followers. Table 2 shows the values of the parameters used in the VFH+ algorithm for obstacle avoidance strategy in Section 4.3, the wheel radius is 0.033 m, the wheel track is 0.287 m, and the sliding mode control parameters are set as $k_1 = k_2 = 2$.

Numeral simulations have been conducted under the above initial conditions, as shown in Figures 5-9. When an obstacle occurs, the AGVs can react promptly to avoid the obstacle and restore the formation, as shown in Figure 5, showing that the formation obstacle avoidance algorithm proposed in this paper is feasible. Figures 6 and 7 demonstrate the distance changes between AGV1, AGV2, and AGV3 along the pre-planned path, especially when a single AGV encounters an obstacle. Eventually, these distances converge,

TABLE 1. VFH+ control

Algorithm 1: Angles update algorithm of the AGVs formation control by integrating artificial potential fields and VFH+ techniques

Step 1. Parameter presetting:

Laser radar resolution: f; b; c_v; M.

Step 2. Initialization:

Initialize the positions of each AGV, $x_c = 0$, $y_c = 0$, $\theta_c = 0$.

Step 3. Implement formation control and obstacle avoidance functionality:

st.1 By scanning surrounding obstacles with a lidar, the following information can be obtained $d^* = \sqrt{(x_{\text{obs}} - x_{\text{AGV}})^2 + (y_{\text{obs}} - y_{\text{AGV}})^2}$, $\alpha = \arctan\left(\frac{y_{\text{obs}} - y_{\text{AGV}}}{x_{\text{obs}} - x_{\text{AGV}}}\right)$, $\alpha \in [0, 2\pi]$.

st.2 The obstacle intensity value m_l for each sector can be calculated as $m_l = c_v^2\,(a - bD_l^2)$.

st.3 Conduct feasibility sector analysis H_l.

st.4 Calculate the optimal avoidance angle using the cost function $C(\vartheta)$.

st.5 Convert α to the corresponding two-dimensional coordinates and calculate the corresponding angular velocity, $\omega_1 = 2 * \sin(\alpha_2)$, where $\alpha_2 = \alpha - \alpha_1$, $\alpha_1 = atan2(\sin(\vartheta) - y_c, \cos(\vartheta) - x_c)$.

Step 4. Iteration:

for $i = 2 : \omega$

st.1 Laser radar scanning,

st.2 **if** $H_i(t) \geq M$

end

else if

st.3 Repeat **Step 3**,

st.4 $\omega(t+1) = \omega_1(t) + \omega(t)$.

end

TABLE 2. Relevant parameters of the VFH+ algorithm in numerical simulations

Parameters	Values	Description
f	1°	Angular resolution
L	4 m	LIDAR measurement distance
d_{safe}	0.01 m	AGV safety distance
μ_1	7	Target direction weight
μ_2	2	Current direction weight
μ_3	2	Previous direction weight

indicating that the distance constraint mechanism effectively ensures the formation of the formation and successfully coordinates the relative positions of the AGVs. This shows that the proposed algorithm not only effectively handles obstacle avoidance but also maintains formation stability in complex environments. Further validation is provided by Figures 8 and 9, which show the changes in the motion angle and speed of the AGVs, confirming the system's stability and responsiveness in dynamic environments.

These experimental results fully validate the feasibility and effectiveness of the proposed formation-based obstacle avoidance algorithm, demonstrating that it can achieve stable operation of the formation control problem of AGVs in practical applications.

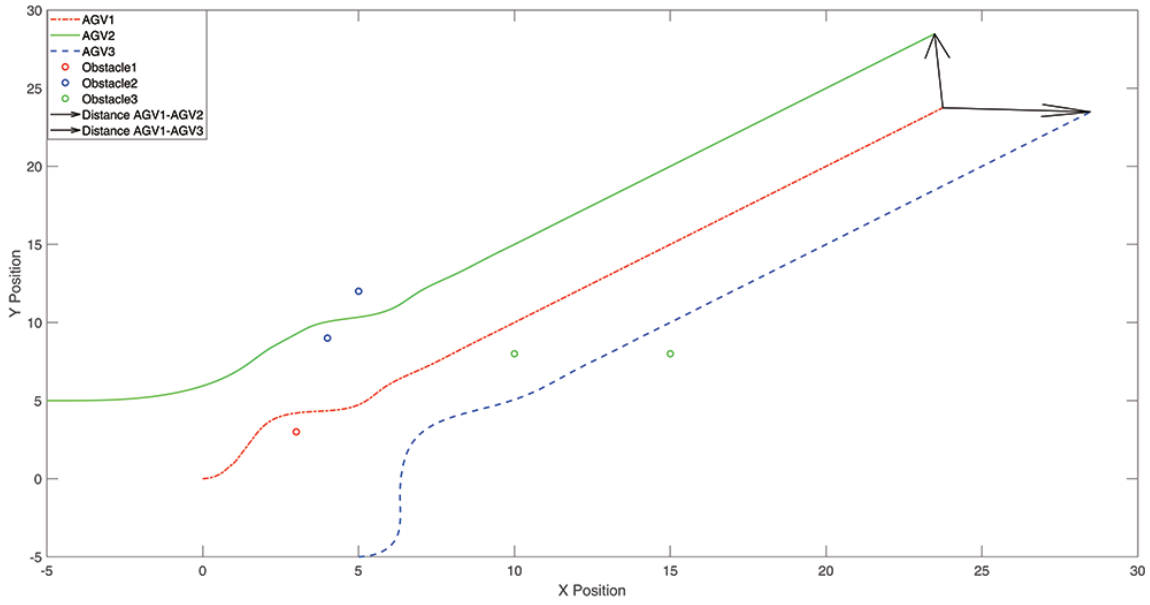

FIGURE 5. Obstacle avoidance process in the formation control problem of AGVs

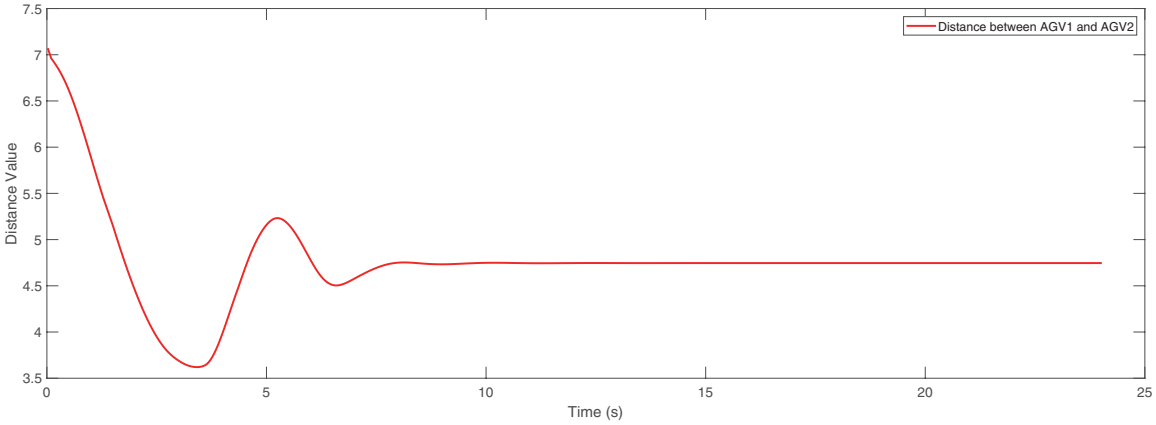

FIGURE 6. The variation of distance between AGV1 and AGV2

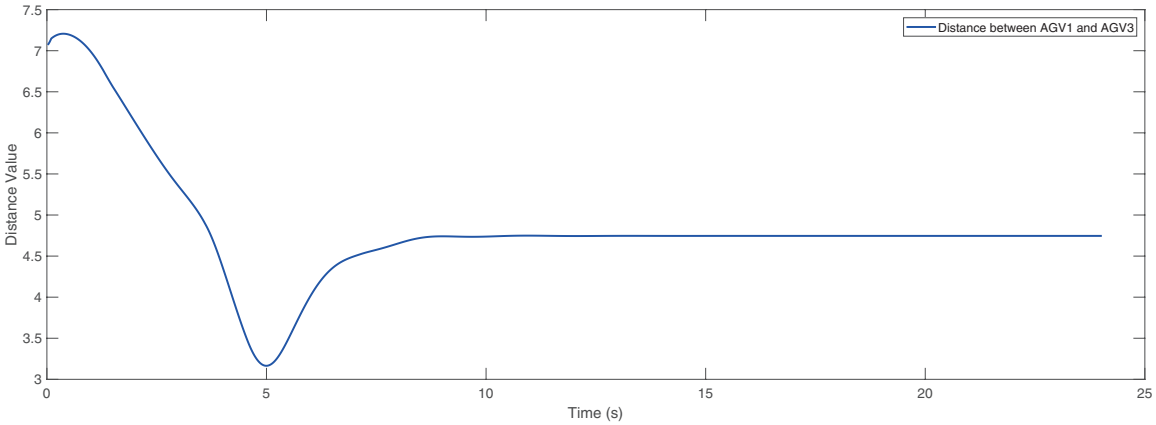

FIGURE 7. The variation of distance between AGV1 and AGV3

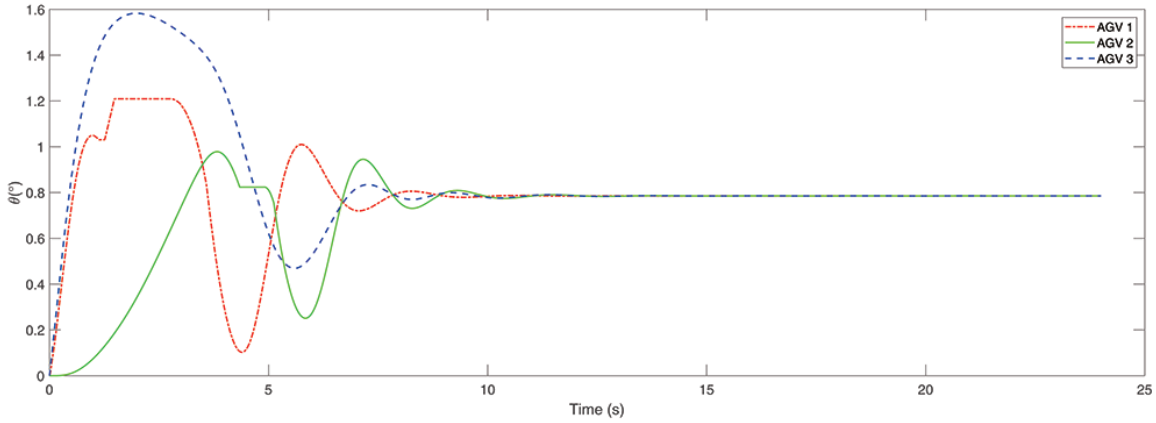

FIGURE 8. The variation of motion angles output by the VFH+ algorithm

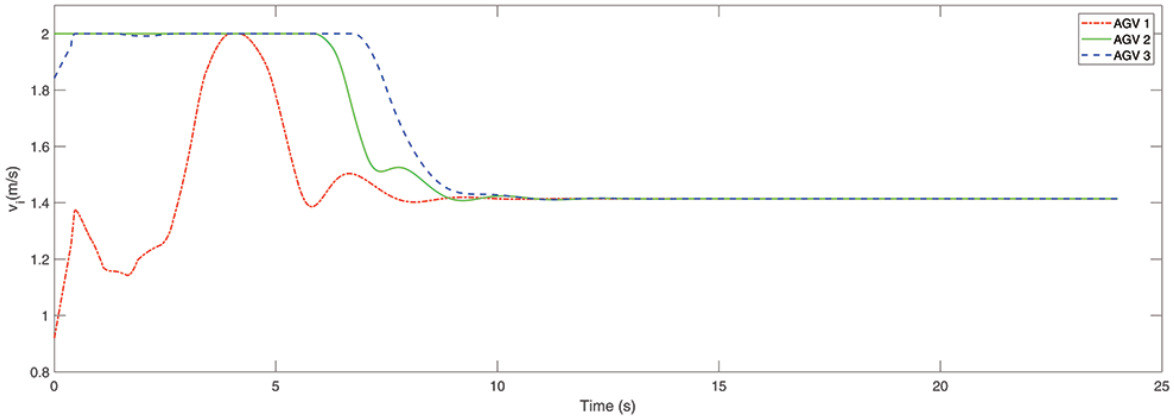

FIGURE 9. The variation of motion speeds output by the VFH+ algorithm

5.2. **Physical experiment.** To further validate the effectiveness of the method proposed in this paper, we have established the hardware platform for formation control of a multi-differential-drive AGV, which mainly includes the XING.YING visual positioning system from NOKOV, a ground station monitoring system, a data transmission system, and the unmanned vehicle system (see PS laboratory images). The unmanned vehicle system employs a model-based system design approach and automatic code generation to deploy the system model onto the hardware. The system model includes sensor data acquisition modules, task management modules, navigation controller modules, motor control modules, ground station data monitoring modules, and distributed communication modules. Reflective balls are installed on the unmanned vehicles, and the XING.YING software reads the position information of the AGV unmanned vehicles during each iteration for corresponding information exchange and target tasking. We still utilize the communication scenario from numerical simulations, conducting experiments on formation obstacle avoidance and collision avoidance with three unmanned vehicles and a randomly positioned obstacle. The experimental parameters for the VFH+ algorithm are consistent with those from the numerical simulation, and Table 3 shows the parameter values of the collision avoidance algorithm in Section 4.2, while Table 4 provides the parameter settings of the kinematic model (2) for the experimental autonomous vehicle, where the angular velocity in (2) can be calculated using the minimum turning radius.

TABLE 3. Collision avoidance algorithm parameter settings

Parameters	Setting values
r_{in}	0.15 m
r_{out}	1 m
k	-2

TABLE 4. AGV operating parameter settings

AGV operating parameters	Setting values
Operating speed	1 m/s
Minimum turning radius	0.1 m

Figure 10 shows snapshots of the obstacle avoidance and collision avoidance experiment with three-differential-drive AGVs. At the beginning of the formation, the AGVs are positioned randomly. After the experiment starts, the AGVs begin to move and form a formation, then follow a pre-defined trajectory (indicated by the red arrows in the figure). During the process, real-time data regarding detected obstacles is continuously acquired, enabling the obstacle avoidance algorithm to dynamically recalculate and optimize a local trajectory for the AGV, thereby ensuring effective navigation around the obstruction. During the return trajectory to the starting point, the dynamically optimized local path maintains the inter-vehicle distance within the predefined safety threshold r_{out}, thereby triggering the collision avoidance mechanism. This strategic path planning ensures safe navigation and prevents potential collisions between the autonomous vehicles, ultimately guiding them back to their initial positions while successfully accomplishing the designated mission. To validate the proposed algorithm's efficacy, we conducted a comparative study consisting of two experimental scenarios: obstacle-present and obstacle-free environments. The experimental results are available for

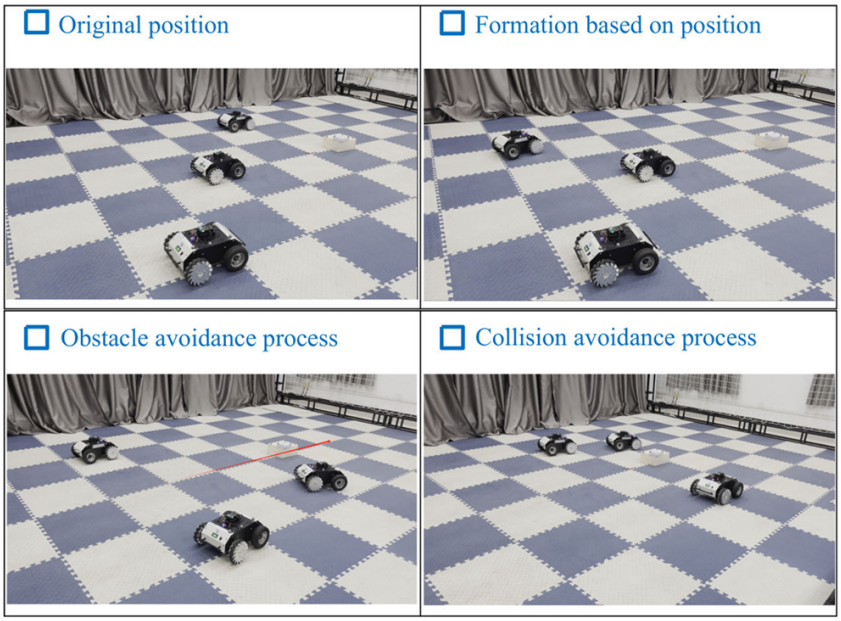

FIGURE 10. Experimental procedure

reference: obstacle scenario (https://youtu.be/Vl_sEf27Wms) and obstacle-free scenario (https://youtu.be/CJ-AF_OjzdA).

Figure 11 presents the repulsive force profiles of the three AGVs during operation. Notably, AGV2 consistently maintained a repulsive force of 0 throughout the entire process, demonstrating its ability to maintain safe distances from other vehicles. The positional dynamics of the AGV system are illustrated in Figures 12 and 13, which respectively depict the trajectory variations along the X and Y axes during the experimental period. Furthermore, Figure 14 demonstrates the angular outputs generated by the VFH+ algorithm, representing the necessary directional adjustments for successful obstacle avoidance by the unmanned vehicles. The system exhibits remarkable performance in three critical aspects: obstacle avoidance precision, path planning, and real-time operational responsiveness. These capabilities are particularly evident in complex environmental scenarios, where the algorithm successfully addresses multiple navigational challenges.

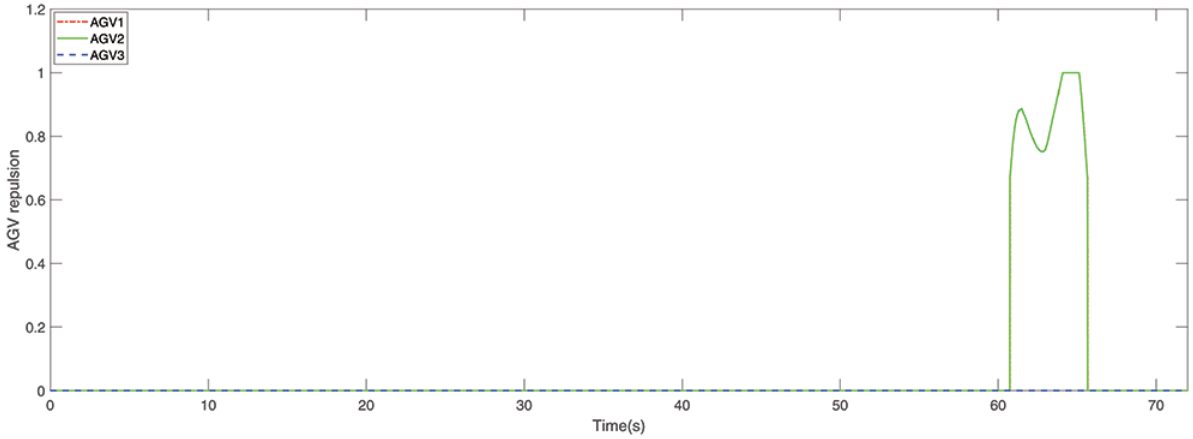

FIGURE 11. Change of repulsive force

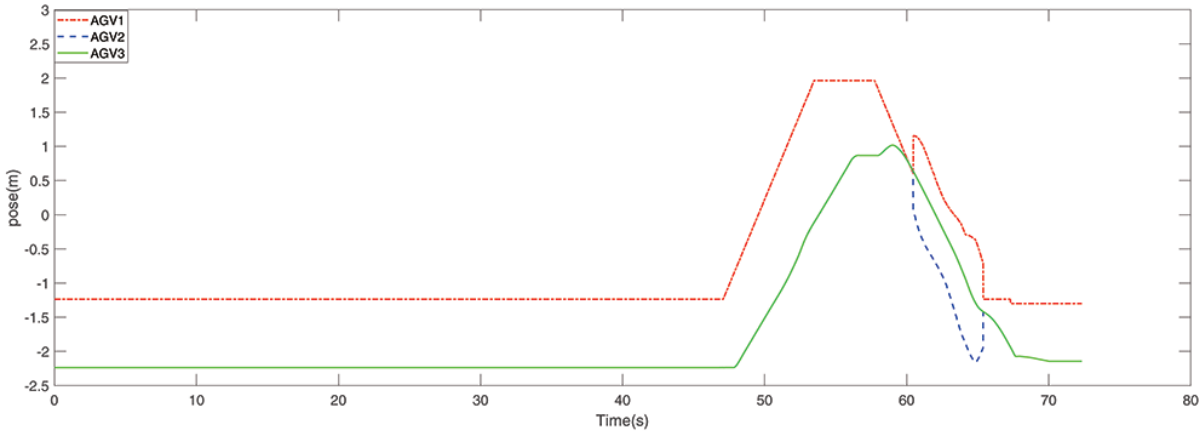

FIGURE 12. Position changes of each AGV in the X direction

Based on these findings, it can be concluded that the proposed algorithm demonstrates significant application potential and substantial practical value for autonomous vehicle navigation systems.

6. **Conclusions.** This paper presents a novel distributed sliding mode control strategy for multi-differential-drive AGVs, specifically designed to address formation control

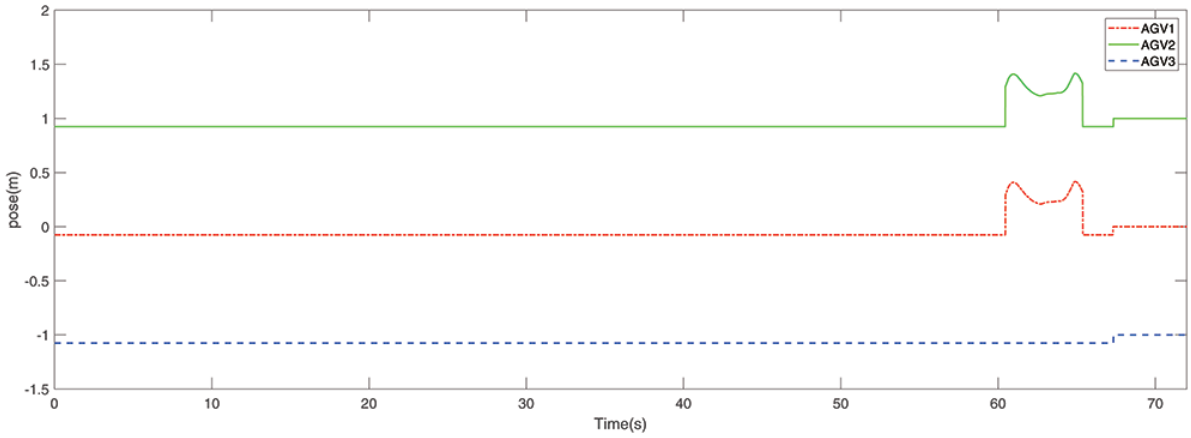

FIGURE 13. Position changes of each AGV in the Y direction

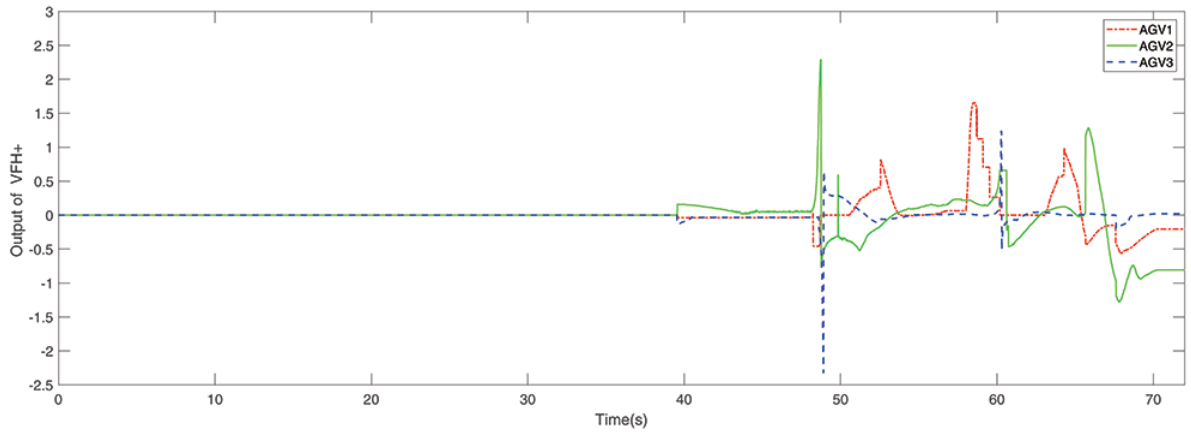

FIGURE 14. Output of the VFH+ algorithm

challenges in complex environments through integrated obstacle avoidance and collision prevention mechanisms. The proposed methodology encompasses three key components: 1) development of a sliding mode controller tailored for the kinematic model of AGVs, 2) implementation of formation shape control via distance-based constraints, and 3) integration of the VFH+ and artificial potential field algorithm for obstacle avoidance and collision prevention. Numerical simulations validate the algorithm's logic and stability, while experimental results on a multi-agent platform demonstrate the system's capability of maintaining leader-follower formations and executing obstacle avoidance with three AGVs. Future work will focus on developing more practical formation obstacle avoidance algorithms for enhanced robustness in complex environments.

Acknowledgment. This work was supported in part by the Science and Technology Research Program of Chongqing Municipal Education Commission under Grant KJZD-K202300807; and in part by the Chongqing Natural Science Foundation under Grant CSTB2024NSCQ-QCXMX0052.

REFERENCES

[1] S. Shao, T. Wang, C. Song, Y. Su, X. Chen and H. Zhao, A novel distributed source seeking method based on multi-robots flocking, *IEEE 9th Annual International Conference on Cyber Technology in Automation, Control, and Intelligent Systems (CYBER)*, Suzhou, China, pp.654-658, 2019.

[2] C. Lin, G. Han, J. Du, Y. Bi, L. Shu and K. Fan, A path planning scheme for AUV flock-based Internet-of-Underwater-Things systems to enable transparent and smart ocean, *IEEE Internet of Things Journal*, vol.7, no.10, pp.9760-9772, 2020.
[3] Y. Xu, H. Lu and Z. Xie, Research on multi-robot cooperative location algorithm based on wireless sensor networks, *International Journal of Innovative Computing, Information and Control*, vol.15, no.5, pp.1779-1792, 2019.
[4] J. Tordesillas and J. P. How, MADER: Trajectory planner in multi-agent and dynamic environments, *IEEE Transactions on Robotics*, vol.38, no.1, pp.463-476, 2022.
[5] C. Huang, Z. Lai, X. Wu and T. Xu, Multimodal locomotion and cargo transportation of magnetically actuated quadruped soft microrobots, *Cyborg and Bionic Systems*, Article ID 0004, 2022.
[6] Y. Liu, H. Chen, Q. Zou, X. Du, Y. Wang and J. Yu, Automatic navigation of microswarms for dynamic obstacle avoidance, *IEEE Transactions on Robotics*, vol.39, no.4, pp.2770-2785, 2023.
[7] S. Shao, J. Zhang, T. Wang, A. Shankar and C. Maple, Dynamic obstacle avoidance algorithm for multi-robot flocking based on improved artificial potential field, *IEEE Transactions on Consumer Electronics*, vol.70, no.1, pp.4388-4399, 2023.
[8] W. Levine and M. Athans, On the optimal error regulation of a string of moving vehicles, *IEEE Transactions on Automatic Control*, vol.11, no.3, pp.355-361, 1966.
[9] J. Wen, J. Yang, Y. Li, J. He, Z. Li and H. Song, Behavior-based formation control digital twin for multi-AUG in edge computing, *IEEE Transactions on Network Science and Engineering*, vol.10, no.5, pp.2791-2801, 2022.
[10] G. Lee and D. Chwa, Decentralized behavior-based formation control of multiple robots considering obstacle avoidance, *Intelligent Service Robotics*, vol.11, pp.127-138, 2018.
[11] Z. Pan, C. Zhang, Y. Xia, H. Xiong and X. Shao, An improved artificial potential field method for path planning and formation control of the multi-UAV systems, *IEEE Transactions on Circuits and Systems II: Express Briefs*, vol.69, no.3, pp.1129-1133, 2021.
[12] X. Dong, B. Yu, Z. Shi and Y. Zhong, Time-varying formation control for unmanned aerial vehicles: Theories and applications, *IEEE Transactions on Control Systems Technology*, vol.23, no.1, pp.340-348, 2014.
[13] X. Wang and G. Yang, Fault-tolerant consensus tracking control for linear multi-agent systems under switching directed network, *IEEE Transactions on Cybernetics*, vol.50, no.5, pp.1921-1930, 2020.
[14] J. Wang, Network-based containment control protocol of multi-agent systems with time varying delays, *International Journal of Innovative Computing, Information and Control*, vol.12, no.6, pp.2089-2098, 2016.
[15] S. Xue, J. Liu, H. Cao, X. Zheng, H. Li and J. Zhang, Leader-following formation tracking of multi-agent systems using adaptive scaling mechanism under spatial constraints, *IEEE Transactions on Systems, Man, and Cybernetics: Systems*, vol.54, no.2, pp.1214-1225, 2024.
[16] N. Gageik, P. Benz and S. Montenegro, Obstacle detection and collision avoidance for a UAV with complementary low-cost sensors, *IEEE Access*, vol.3, pp.599-609, 2015.
[17] S. Vargas, H. M. Becerra and J. Hayet, MPC-based distributed formation control of multiple quadcopters with obstacle avoidance and connectivity maintenance, *Control Engineering Practice*, vol.121, 105054, 2022.
[18] Y. Lin and S. Saripalli, Sampling-based path planning for UAV collision avoidance, *IEEE Transactions on Intelligent Transportation Systems*, vol.18, no.11, pp.3179-3192, 2017.
[19] Q. Jia, Obstacle avoidance path planning of space manipulator based on A* algorithm, *Journal of Engineering Mechanics*, vol.46, pp.109-115, 2010.
[20] G. Surname, J. Huang, S. Wu and R. Fan, Obstacle avoidance algorithm of simulation robotic fish based on ant colony algorithm, *Chinese Automation Congress (CAC)*, Shanghai, China, pp.3461-3464, 2020.
[21] W. Ning, J. Dai, Y. Jin, Y. Li and L. Lu, Multi-UAV trajectory planning simulation based on adaptive extended potential field, *Journal of System Simulation*, vol.33, no.9, pp.2147-2156, 2021.
[22] I. Ulrich and J. Borenstein, VFH+: Reliable obstacle avoidance for fast mobile robots, *IEEE International Conference on Robotics and Automation*, Leuven, Belgium, vol.2, pp.1572-1577, 1998.
[23] H. A. Neamah, E. Donát and P. Korondi, Optimizing autonomous navigation in unknown environments: A novel trap avoiding vector field histogram algorithm VFH+T, *Results in Engineering*, vol.23, 102625, 2024.
[24] Y. Zhang, J. Chen, M. Chen, C. Chen, Z. Zhang and X. Deng, Integrated the artificial potential field with the leader-follower approach for unmanned aerial vehicles cooperative obstacle avoidance, *Mathematics*, vol.12, no.7, 954, 2024.

[25] J. González-Sierra, E. G. Hernández-Martínez, M. Ramírez-Neria and G. Fernandez-Anaya, Smooth collision avoidance for the formation control of first order multi-agent systems, *Robotics and Autonomous Systems*, vol.165, 104433, 2023.
[26] X. Fu, C. Zhi and D. Wu, Obstacle avoidance and collision avoidance of UAV swarm based on improved VFH algorithm and information sharing strategy, *Computers & Industrial Engineering*, vol.186, 109761, 2023.
[27] G. Wang, X. Wang and S. Li, A guidance module based formation control scheme for multi-mobile robot systems with collision avoidance, *IEEE Transactions on Automation Science and Engineering*, vol.21, no.1, pp.382-393, 2024.
[28] X. Wang, W. Liu, Q. Wu and S. Li, A modular optimal formation control scheme of multi-agent systems with application to multiple mobile robots, *IEEE Transactions on Industrial Electronics*, vol.69, no.9, pp.9331-9341, 2022.
[29] Y. Tang, Z. Deng and Y. Hong, Optimal output consensus of high-order multi-agent systems with embedded technique, *IEEE Transactions on Cybernetics*, vol.49, no.5, pp.1768-1779, 2019.
[30] H. Guo, F. Liu, R. Yu, Z. Sun and H. Chen, Regional path moving horizon tracking controller design for autonomous ground vehicles, *Science China Information Sciences*, vol.60, pp.1-7, 2017.
[31] D. Díaz and L. Marín, VFH+D: An improvement on the VFH+ algorithm for dynamic obstacle avoidance and local planning, *IFAC-PapersOnLine*, vol.53, no.2, pp.9590-9595, 2020.
[32] K. D. Sharma, A. Chatterjee and A. Rakshit, A PSO-Lyapunov hybrid stable adaptive fuzzy tracking control approach for vision-based robot navigation, *IEEE Transactions on Instrumentation and Measurement*, vol.61, no.7, pp.1908-1914, 2012.
[33] R. E. Aráujo and D. S. Freitas, Non-linear control of an induction motor: Sliding mode theory leads to robust and simple solution, *International Journal of Adaptive Control and Signal Processing*, vol.14, nos.2-3, pp.331-353, 2000.

Author Biography

Huiyan Zhang received the M.Sc. degree in Control Engineering and the Ph.D. degree in Control Theory and Control Engineering from Harbin Institute of Technology, Harbin, in September 2014 and April 2019, respectively. From September 2015 to September 2017, she was a Joint Training Ph.D. Student with the School of Electrical and Electronic Engineering, the University of Adelaide. She is currently an Associate Professor with Chongqing Technology and Business University. Her research interests include multi-agent systems, stochastic switched systems, event-triggered scheme, robust control, etc.

Dr. Zhang serves as an Associate Editor for several journals, including IEEE Transactions on Cybernetics, Signal Processing, and Journal of the Franklin Institute.

Yu Huang received her Bachelor of Engineering degree in Automotive Service Engineering from Chongqing University of Technology, China, in 2023. She is currently a master's student in Mechanical Manufacturing and Automation at Chongqing Technology and Business University, Class of 2023. Her primary research interest is multi-agent systems cooperative control.

Xiaoli Chen is currently an undergraduate in the Chongqing Engineering Laboratory for Detection Control and Integrated Systems at Chongqing Technology and Business University, majoring in Automation. Her primary research interest lies in the development of advanced control strategies for Automated Guided Vehicles (AGVs) with obstacle avoidance capabilities.

Jiangyan Zou received her Bachelor of Management degree in Human Resource Management from the School of Management at Chongqing University of Technology, China, in 2023. She is currently a master's student in Computer Technology at Chongqing Technology and Business University, China. Her primary research interest is visual SLAM in computer vision.

Wenting He received her Bachelor of Engineering degree in Computer Science and Technology from Chongqing Technology and Business University in 2022. She is currently a master's student in Artificial Intelligence at Chongqing Technology and Business University, Class of 2024. Her primary research interest is adaptive control of automotive suspension systems based on neural networks.